Batteries & Supercaps

Research Article
doi.org/10.1002/batt.202400776

Chemistry Europe
European Chemical Societies Publishing

www.batteries-supercaps.org

Polyacrylic Acid-Modified Gel Electrolytes for Enhanced Electrochemical Performance in Aqueous Zinc Batteries

Yuguo Zheng,[a] Jiaxian Zheng,[a] and Hanfeng Liang*[a]

Gel electrolytes are widely used in aqueous zinc batteries to alleviate water-related issues. In this study, we develop a new gel electrolyte by introducing a small amount of polymer additive, inspired by electrolyte additives in liquid electrolytes. The introduction of polyacrylic acid (PAA) additive improves the ionic diffusion coefficient inside the gel electrolyte and enables uniform Zn deposition, enhancing the reversibility of Zn batteries. As a result, the Zn||$Mg_{0.1}V_2O_5$ batteries using the modified electrolyte show a maximum capacity of 300 mAh g^{-1} at a current density of 0.5 A g^{-1} and remain stable over 300 cycles. In contrast, the batteries without the PAA additive suffer from rapid capacity decay within 150 cycles under the same conditions. This study presents a simple and cost-effective method of gel electrolyte additive engineering to enhance the performance of aqueous zinc batteries.

Introduction

As global energy demands continue to rise and the deployment of sustainable green energy sources such as wind and solar power expands, the need for efficient and cost-effective large-scale energy storage technologies become more critical. While traditional lithium-ion batteries (LIBs) are widely used for small-scale energy storage and portable devices, their high costs and potential safety risks pose significant challenges for their large-scale energy storage solutions. This drives the urgent need for alternative technologies that offer greater safety, environmental sustainability, and cost-effectiveness. Aqueous zinc-ion batteries (AZIBs) have emerged as a promising solution due to their use of water as the electrolyte and the abundant availability of zinc metal.[1–3] Compared to LIBs, AZIBs offer clear advantages in terms of safety, environmental friendliness, and cost control, particularly for large-scale energy storage applications. Despite these benefits, the commercialization of aqueous zinc-ion batteries is hindered by challenges such as the dissolution of cathode active materials and the growth of zinc dendrites on the anode, which negatively impact cycle stability and overall battery performance.[4]

To enhance the cycling stability of AZIBs, researchers have been exploring the use of hydrogel electrolytes as alternatives to traditional aqueous electrolytes, thereby eliminating the need for separators (Scheme 1).[5] Hydrogel electrolytes, which function as quasi-solid-state electrolytes, comprise an organic polymer network that contains water molecules and zinc salts.[6] The functional groups on the polymer backbone form hydrogen bonds with water molecules, reducing the free water content, and interact with zinc ions (Zn^{2+}), facilitating their diffusion and conductivity. This structure endows hydrogel electrolytes with high ionic conductivity and the ability to suppress side reactions, making them a popular choice in AZIB research.[7] Common hydrogel electrolyte materials include polyacrylamide (PAM),[8] polyvinyl alcohol (PVA),[9] and polyacrylic acid (PAA),[10] *etc.* Despite the design of various types of gel electrolytes, further improvements are still needed in terms of electrode interface stability and cycle life.[11] There is an urgent need for a simple and cost-effective method to optimize and enhance gel electrolytes performance. In traditional aqueous zinc batteries, small amounts of electrolyte additives are often used in the liquid electrolyte to improve electrode interface stability and suppress dendrite growth at a low cost.[12–14]

Inspired by this approach, the present study focuses on the design of a hydrogel electrolyte based on polyacrylamide (AM). We introduce a small amount of polyacrylic acid (PAA), a polymer with the same backbone structure but containing carboxyl groups, as an electrolyte additive, systematically analyzing its effect on electrochemical performance. Through comprehensive evaluation, we found that the performance of the gel electrolyte significantly improved after the addition of PAA polymer with carboxyl groups. Both the Zn||Zn symmetric cells and Zn||$Mg_{0.1}V_2O_5$ full batteries showed enhanced performance. Specifically, the Zn||$Mg_{0.1}V_2O_5$ batteries achieved a high capacity of 300 mAh g^{-1} and maintained stable cycling for 300 cycles at a current density of 0.5 A g^{-1}, whereas the unmodified batteries only maintained a maximum capacity of 200 mAh g^{-1} and experienced rapid capacity decay after 100 cycles.

Results and Discussion

The gel electrolyte without polyacrylic acid (PAA) was prepared by photo-induced polymerization of acrylamide (AM) monomers with $Zn(OTf)_2$) aqueous solution (denoted as "w/o PAA"). Building on this, 1 wt% of carboxylated polyacrylic acid (PAA) polymer was incorporated as an additive during the preparation

[a] *Y. Zheng, J. Zheng, Prof. H. Liang*
State Key Laboratory of Physical Chemistry of Solid Surfaces, College of Chemistry and Chemical Engineering
Xiamen University
Xiamen (361005) China
E-mail: hfliang@xmu.edu.cn

Research Article
doi.org/10.1002/batt.202400776
Chemistry Europe
European Chemical Societies Publishing

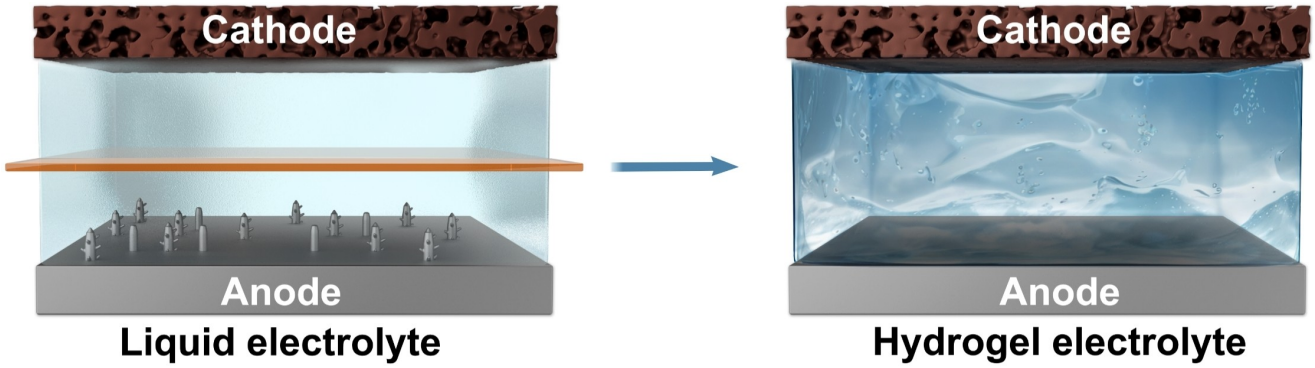

Scheme 1. Comparison between liquid and hydrogel electrolytes in alleviating side reactions and Zn dendrites.

process to obtain the modified gel electrolyte (denoted as "PAA"). PAA, which is rich in carboxyl groups, was selected due to its structural compatibility with PAM, as both polymers share similar chain segment structures. Under ultraviolet (UV) light, PAM and PAA undergo crosslinking, with the formation of hydrogen bonds between them. This crosslinked hydrogel polymer framework contains abundant amide and carboxyl functional groups, which are capable of forming hydrogen bonds with water molecules, thereby reducing the content of free water and suppressing the associated side reactions. Additionally, the carboxyl groups (–COOH) in PAA additive interact with Zn^{2+} ions, modifying their solvation structure. This interaction promotes the rapid conduction of Zn^{2+} ions within the electrolyte, which, in turn, enhances the overall performance of the battery by facilitating more efficient Zn^{2+} ion transport and improving electrode processes (Figure 1a). To demonstrate the successful incorporation of PAA into the PAM gel electrolyte, Fourier-transform infrared (FTIR) spectroscopy was used to characterize the structural features of the two gel electrolytes. For the gel electrolyte without PAA, the FTIR spectrum shows typical C=O and O–H stretching vibration absorption peaks at 1633 and 3300 cm^{-1}, respectively. Addition-

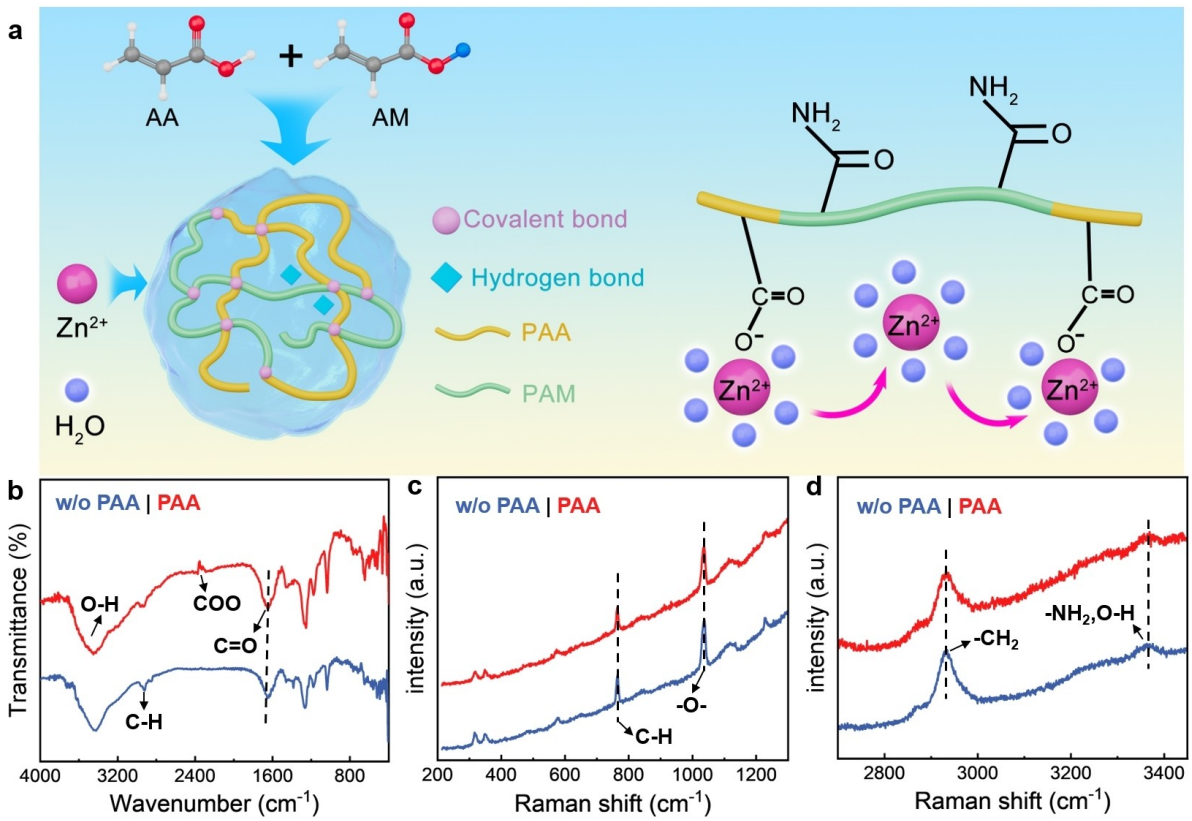

Figure 1. (a) Mechanism diagram of the role of PAA additive in the PAM gel electrolyte. (b) FT-IR and (c, d) Raman spectra of the gel electrolyte without and with PAA.

Research Article
doi.org/10.1002/batt.202400776
Chemistry Europe
European Chemical Societies Publishing

ally, a symmetric C–H stretching vibration peak at 2923 cm^{-1} was observed, indicating the presence of -CH_2- groups and confirming the successful polymerization of the AM monomer into PAM. In the PAA gel electrolyte, the C=O stretching vibration peak shifts slightly to 1630 cm^{-1}, further indicating the incorporation of PAA into the system (Figure 1b).[15–16] This shift can be attributed to the introduction of carboxyl groups from PAA, which form additional hydrogen bonds with other groups in the gel electrolyte, thereby causing the C=O peak to shift to a lower wavenumber. Additionally, a stretching vibration peak for COO was detected at 2360 cm^{-1} providing further evidence of the successful incorporation of PAA into the system. Raman spectrum of the gel electrolyte without PAA reveals characteristic peaks at 1034, 2929 and 3300 cm^{-1} attributed to the stretching vibrations of ether (–O–) bonds, methylene group (–CH_2), and hydroxyl (O–H) or amine (–NH_2) groups, respectively (Figure 1c-d).[17–18] Additionally, a bending vibration peak of C–H was observed at 764 cm^{-1}, further confirming the presence of –CH_2– groups. While the ether bond stretching vibration peak of the PAA gel electrolyte slightly shifts to 1037 cm^{-1}, indicating enhanced intermolecular interactions, particularly through the formation of additional hydrogen bonds due to the addition of PAA. These results confirm the successful incorporation of PAA additive into the gel electrolyte.

Firstly, we optimized the content of the PAA additive and assembled Zn||Cu half-symmetric cells for performance testing with PAA contents of 1, 5, 10, and 20 wt%. We found that the cell with 1 wt% PAA exhibited the best performance, maintaining a stable operation for over 200 cycles while retaining 100% Coulombic efficiency. In contrast, cells with other PAA concentrations could only sustain lower Coulombic efficiencies and deactivated within 40 cycles (Figure 2a). Therefore, we chose 1 wt% as the optimal additive concentration. To further investigate the role of PAA additive, we assembled Zn||Zn symmetric batteries and tested them at a current density of 2 mA cm^{-2}. The result shows that Zn||Zn symmetric batteries with PAA gel electrolyte maintains stable cycling for 150 h, whereas those with electrolyte without PAA fails within 50 h (Figure 2b). We further evaluated the Coulombic efficiency (CE) using Zn||Cu half-cells. The half-cell with PAA gel electrolyte maintains 100% CE while operating stably for over 210 h, whereas the half-cell with no PAA fails within 100 h (Figure 2c). To investigate the effect of PAA additive on ionic conductivity, we assembled SS||SS symmetric cells and measured the ion conductivities of two gel electrolytes. The results show that the ionic conductivity of the pristine gel electrolyte is 2.78×10^{-5} S cm^{-1}, while that of the PAA gel electrolyte is 3.95×10^{-5} S cm^{-1}. This indicates that the introduction of the PAA additive significantly enhances the ionic conductivity of the gel electrolyte, which can be attributed to the large number of carboxyl groups in PAA that facilitate the conduction of Zn^{2+} ions within the electrolyte (Figure 2d). The significant improvement in cycling life is primarily attributed to the carboxyl groups in PAA, which can coordinate with Zn^{2+} ions, facilitating

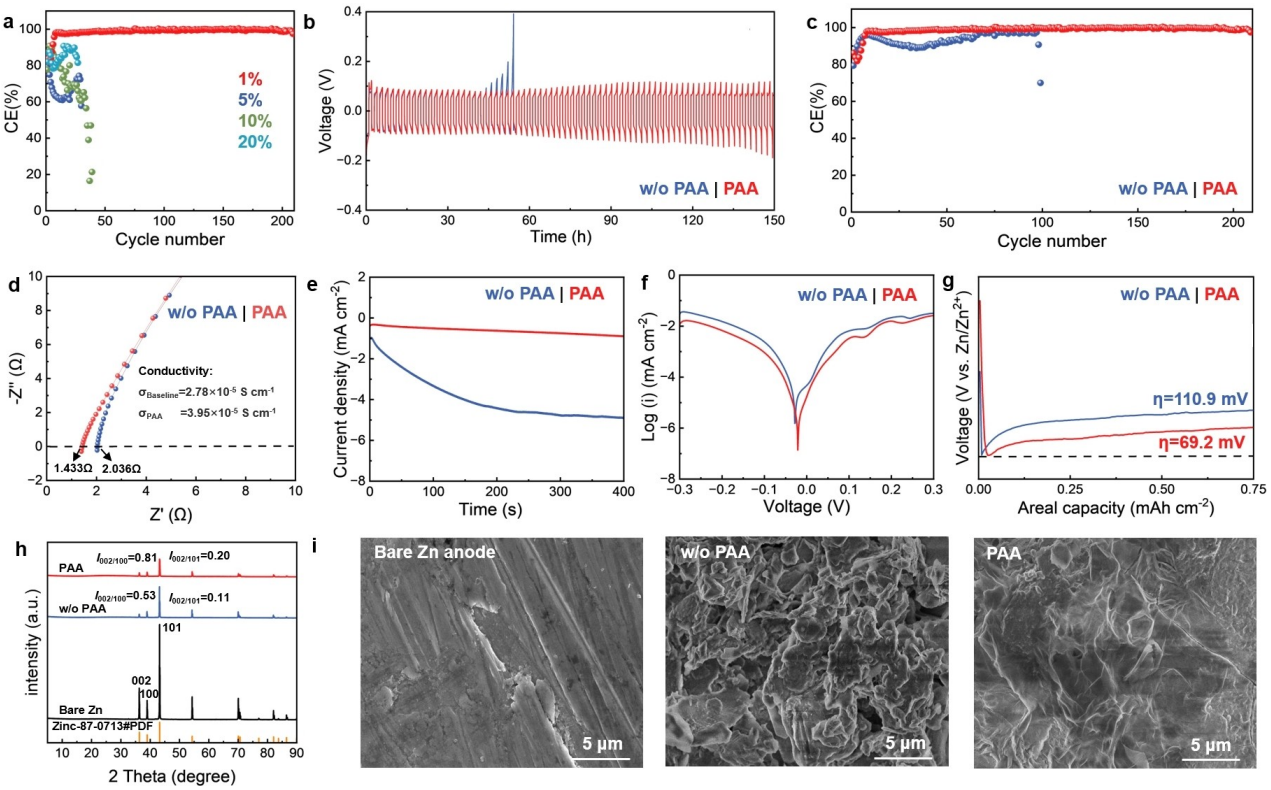

Figure 2. (a) Coulombic efficiencies of Zn||Cu asymmetric cells tested at 2 mA/mAh cm^{-2}. (b) Cycling performance of Zn||Zn symmetric cells at 2 mA/mAh cm^{-2}. (c) Coulombic efficiencies of Zn||Cu asymmetric cells tested at 2 mA/mAh cm^{-2}. (d) Ionic conductivity of the gel electrolyte. (e) I-t curves, (f) Tafel curves, and (g) nucleation overpotentials of the Zn anodes. (h) XRD pattern of the anode. (i) SEM images of the Zn anodes in Zn||Zn symmetric cells after 50 h cycling at 2 mA/mAh cm^{-2}.

Research Article
doi.org/10.1002/batt.202400776
Chemistry Europe
European Chemical Societies Publishing

uniform deposition of Zn^{2+} on the Zn anode and suppressing side reactions.[19–20] Specifically, the chronoamperometry (CA) of Zn anode with the pristine gel electrolyte reveals a rapid initial decrease in current density, suggesting a quick initial diffusion of Zn^{2+} ions, followed by a stabilization (Figure 2e). This behavior indicates that the diffusion process is more 2D in nature, where ions primarily move along the surface plane, leading to less stable and uniform deposition over time. While more stable current density and slight decrease in the CA curve of Zn anode with PAA electrolyte suggest a controlled, continuous diffusion process, indicative of 3D diffusion. This behavior promotes a uniform distribution of Zn^{2+} ions throughout the electrolyte, reducing localized high concentrations and mitigating dendrite growth and localized corrosion.[21] Tafel plots demonstrate that the Zn anode with PAA electrolyte possess a lower corrosion current and a higher corrosion voltage (Figure 2f), suggesting enhanced anti-corrosion property. In addition, the Zn nucleation overpotential in the gel electrolyte with PAA is smaller than that without PAA (Figure 2g), leading to a more uniform Zn deposits.[22] Additionally, we have performed X-ray diffraction (XRD) measurements of the Zn electrode after 50 hours of cycling. The results show a significant change in the diffraction peak intensities: in the PAA-containing electrolyte, the $I_{002/100}$ ratio is 0.81 and $I_{002/101}$ is 0.20, which are notably higher than the values observed in the pristine electrolyte ($I_{002/100}=0.53$, $I_{002/101}=0.11$). This suggests that in the presence of PAA, Zn^{2+} tends to preferentially deposit on the (002) crystallographic plane, promoting more uniform deposition of Zn^{2+} and effectively inhibiting the growth of zinc dendrites (Figure 2h). Indeed, scanning electron microscopy (SEM) images reveal that the Zn anode with PAA electrolyte exhibits a smoother surface than that without PAA (Figure 2i).

We then assembled Zn||$Mg_{0.1}V_2O_5$ full batteries using $Mg_{0.1}V_2O_5$ (MVO) as the cathode (Figure 3a,b) with either the gel electrolyte with or without PAA to evaluate the impact of the PAA additive on electrochemical performance. The cyclic voltammetry (CV) curves of both batteries exhibit similar redox peaks (Figure 3c), indicating that the PAA additive does not alter the Zn (de)intercalation chemistry.[23] The comparable CV areas suggest that both batteries have similar initial capacities. However, as cycling progresses, the specific capacity differences become more pronounced (Figure 3d). At a current density of 0.5 A g^{-1}, both batteries show an "activation process", where the capacity gradually increases to a maximum value.[24] This process primarily arises from solid (cathode)-quasi solid (gel electrolyte) interfaces requiring additional energy to overcome the diffusion barriers.[25] Unlike in liquid electrolytes, where H_2O and Zn^{2+} can rapidly and abundantly diffuse to the cathode, the diffusion process in the gel electrolyte is slower, leading to a gradual activation. It is noted that the battery with PAA electrolyte requires a longer "activation process".

This is because the carboxyl groups in the PAA additive can form hydrogen bonds with H_2O, reducing the amount of active water and binding with Zn^{2+}, thereby limiting the diffusion of H_2O and Zn^{2+}. As a result, the battery with PAA gel electrolyte has a longer "activation process". Nonetheless, the battery with PAA gel electrolyte achieves a maximum capacity of 300 mAh g^{-1} and maintains stable cycling over 300 cycles, while the battery with pristine gel electrolyte only reaches a maximum capacity of 200 mAh g^{-1}, and experiences rapid capacity degradation within 100 cycles due to side reactions. This indicates that the addition of PAA additives enhances both the capacity and cycling stability of the full battery.

To investigate the effect of PAA additives on the diffusion of Zn^{2+} ions within gel electrolytes, we employed the galvano-

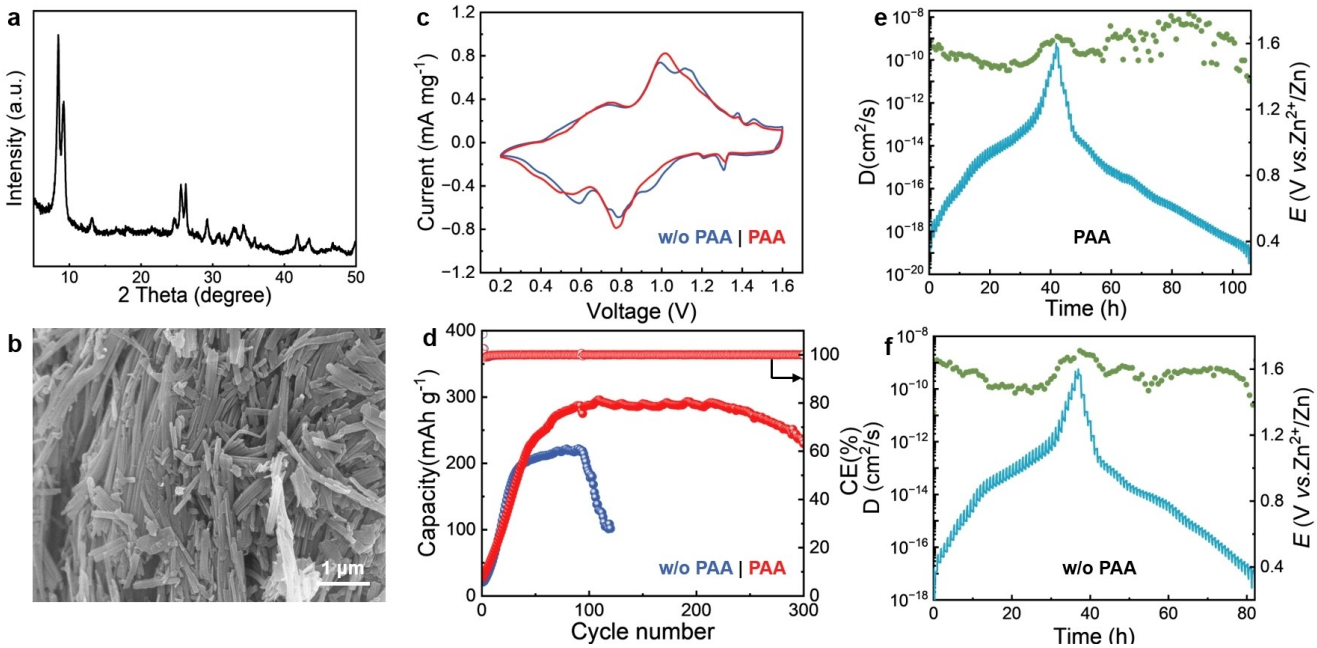

Figure 3. (a) XRD pattern and (b) SEM image of MVO. (c) CV curves and (d) cycling performance at 0.5 A g^{-1} of MVO. GITT curves of the batteries with (e) PAA gel electrolyte and (f) the gel electrolyte without PAA.

Research Article
doi.org/10.1002/batt.202400776
Chemistry Europe
European Chemical Societies Publishing

static intermittent titration technique (GITT) to systematically measure the ion diffusion coefficients for Zn||MVO batteries with the gel electrolyte with or without PAA. The results show that both batteries have similar ion diffusion coefficients of approximately 10^{-10} S cm^{-1} during the charging process. However, during the discharge process, the ion diffusion coefficient of the battery with PAA gel electrolyte can reach as high as 10^{-8} S cm^{-1} (Figure 3e), while that without PAA is only 10^{-9} S cm^{-1} (Figure 3f), indicating that the PAA additives enhance the transport of Zn^{2+} ions within the gel electrolyte.[26] This enhancement is due to the carboxyl groups of PAA, which act as Zn^{2+} transport sites, facilitating the conduction and diffusion of Zn^{2+} ions within the gel electrolyte. These results collectively demonstrate that the carboxyl groups not only improve the transport properties of Zn^{2+} ions within the gel electrolyte but also promote the uniform deposition of Zn^{2+} on the anode.

To identify the effect of PAA additives in stabilizing the Zn anode and the MVO cathode, we fabricated a Janus gel electrolyte, with one side consisting of the pristine gel electrolyte without PAA and the other side a PAA gel electrolyte (Figure 4a **inset**). We assembled a Zn||Cu half-cell and conducted tests at a current density of 2 mA cm^{-2}. The results show that the anode-PAA|PAA -cathode gel electrolyte can stably cycle for 210 h with 100% coulombic efficiency, while samples with w/o PAA gel electrolyte on either the Zn anode or Cu cathode side fail within 30 h, exhibiting low Coulombic efficiencies (Figure 4a). A similar phenomenon is observed in full batteries. Long-cycle performance tests on Zn||MVO full batteries reveal that, at a current density of 0.5 A g^{-1}, the battery with anode-PAA|PAA-cathode gel electrolyte maintains a high capacity of 215 mAh g^{-1} after 300 cycles. In contrast, the battery with PAA only in the anode side exhibits rapid capacity degradation after 120 cycles, and the battery with PAA only in the cathode side quickly lost capacity after only 30 cycles. This result suggests that the PAA additive is more effective in stabilizing Zn anodes. Notably, the battery performance with latter is even worse than the former (Figure 4b). This is because the different compositions of the gel electrolyte with and without PAA create an additional interface within the Janus gel electrolyte, thereby affecting ion transport.

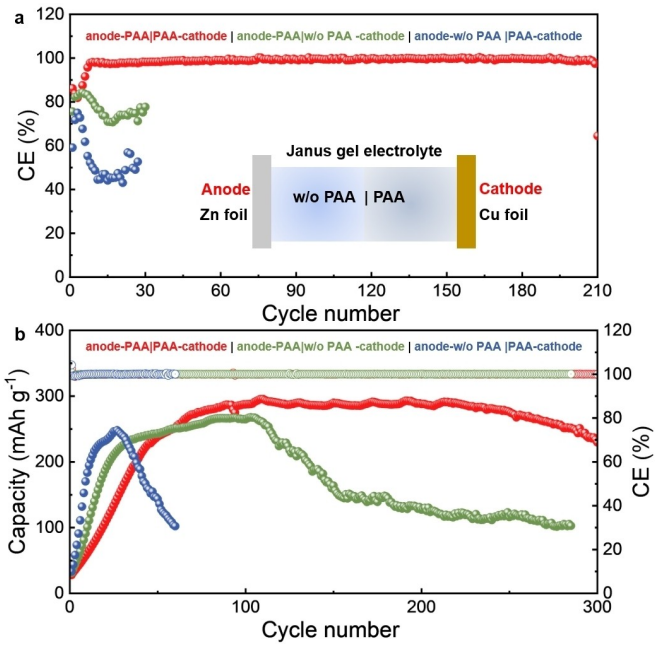

Figure 4. (a) Coulombic efficiencies (CEs) of Zn||Cu asymmetric cells tested at 2 mA/mAh cm^{-2}. (b) Cycling performance at 0.5 A g^{-1} of the batteries with Janus gel electrolyte

Conclusions

This work investigates the impact of PAA electrolyte additives on gel electrolytes, demonstrating that even a small amount of PAA additive can effectively enhance the zinc battery performance. On the cathode side, PAA modulates the solvation structure of Zn^{2+}, promoting efficient insertion and extraction. On the anode side, PAA facilitates uniform Zn^{2+} deposition, suppresses side reactions, and inhibits the growth of zinc dendrites. As a result, the Zn||$Mg_{0.1}V_2O_5$ batteries with PAA gel electrolyte achieved a maximum capacity of 300 mAh g^{-1} at a current density of 0.5 A g^{-1} and remained stable over 300 cycles, outperforming the batteries without PAA additives.

Experimental Section

Synthesis of $Mg_{0.1}V_2O_5$ (MVO) Nanobelts

The MVO nanobelts were synthesized using a simple hydrothermal method. In a typical procedure, 2 mmol of magnesium acetate, 4 mmol of ammonium metavanadate, and 10 mL of acetic acid were added to 40 mL of deionized water and continuously stirred magnetically at 80 °C until completely dissolved. The resulting solution was then transferred to a 100 mL Teflon-lined stainless-steel autoclave and maintained at 180 °C for 48 hours. Finally, the MVO were thoroughly washed with deionized water and dried at 60 °C for 12 hours.

Synthesis of Gel Electrolytes

The gel electrolyte without PAA was synthesized using a straightforward photopolymerization method. Initially, 0.75 g of acrylamide (99.9%), 0.726 g of zinc trifluoromethanesulfonate (98%), 2.5 mg of 2-hydroxy-4-(2-hydroxyethoxy)-2-methylpropiophenone (Irgacure 2959) and 1.5 mg of N,N′-methylene-bis(acrylamide) were dissolved in 2 mL of deionized water and sonicated until fully dissolved. Finally, the precursor solution was transferred into a designated mold, and the gel electrolyte was obtained after 2 minutes of UV exposure. In addition, 1 wt% polymer additives of polyacrylic acid (2000 g mol^{-1}) were added into the pristine hydrogel electrolyte to form the corresponding gel electrolyte.

Material Characterization

Scanning electron microscopy (SEM, Hitachi S-4800, Japan) was employed to characterize the morphologies. The crystal structures were probed *via* X-ray diffraction (XRD, Rigaku IV, Japen) measurements with a scan rate of 10° min^{-1}. Fourier-transform infrared spectroscopy (FTIR, Nicolet iS50, USA) was used to probe molecular

structures and chemical bondings. Raman spectra were collected using an XploRA plus (HORIBA) spectroscope.

Electrochemical Measurements

The cyclic voltammetry (CV) curves were collected on a CHI760E (CH Instruments, Shanghai) electrochemical workstation within the potential range of 0.2 to 1.6 V at room temperature. Linear sweep voltammetry (LSV) curves were recorded at a scan rate of 1 $mV s^{-1}$. Tafel curves were recorded at a scan rate of 0.01 $V s^{-1}$. The galvanostatic charge and discharge (GCD) tests of the cells were carried out on a NEWARE Battery Test System (CT-4008Tn-5V20mA-164, Shenzhen, China), with a potential range of 0.2 to 1.6 V. The galvanostatic intermittent titration technique (GITT) was performed with the voltage window of 0.2 to 1.6 V at a constant current of 30 $mA g^{-1}$, and the current pulse time and the relaxation time were both 10 mins.

Acknowledgements

This work was supported by the Fujian Provincial Science and Technology Program for External Cooperation (2024I0001) and the Fundamental Research Funds for the Central Universities of China (Grant No.: 20720240066).

Conflict of Interests

The authors declare no conflict of interest.

Data Availability Statement

The data that support the findings of this study are available from the corresponding author upon reasonable request.

Keywords: zinc batteries · hydrogel electrolyte · functional group · PAA

[1] X. Yu, Z. Li, X. Wu, H. Zhang, Q. Zhao, H. Liang, H. Wang, D. Chao, F. Wang, Y. Qiao, H. Zhou, S.-G. Sun, *Joule* **2023**, *7*, 1145–1175.
[2] J. Zheng, X. Liu, Y. Zheng, A. N. Gandi, X. Kuai, Z. Wang, Y. Zhu, Z. Zhuang, H. Liang, *Nano Lett.* **2023**, *23*, 6156–6163.
[3] J. Zheng, Y. Wu, H. Xie, Y. Zeng, W. Liu, A. N. Gandi, Z. Qi, Z. Wang, H. Liang, *ACS Nano* **2023**, *17*, 337–345.
[4] Y. Dai, C. Zhang, J. Li, X. Gao, P. Hu, C. Ye, H. He, J. Zhu, W. Zhang, R. Chen, W. Zong, F. Guo, I. P. Parkin, D. J. L. Brett, P. R. Shearing, L. Mai, G. He, *Adv. Mater.* **2024**, *36*, 2310645.
[5] F. Chen, X. Li, Y. Yu, Q. Li, H. Lin, L. Xu, H. C. Shum, *Nat. Commun.* **2023**, *14*, 2793–2793.
[6] J. Chong, C. Sung, K. S. Nam, T. Kang, H. Kim, H. Lee, H. Park, S. Park, J. Kang, *Nat. Commun.* **2023**, *14*, 2206.
[7] H. Peng, D. Wang, F. Zhang, L. Yang, X. Jiang, K. Zhang, Z. Qian, J. Yang, *ACS Nano* **2024**, *18*, 21779–21803.
[8] Y. Liu, A. Gao, J. Hao, X. Li, J. Ling, F. Yi, Q. Li, D. Shu, *Chem. Eng. J.* **2023**, *452*, 139605.
[9] J. Zhou, Y. Mei, F. Wu, Y. Hao, W. Ma, L. Li, M. Xie, R. Chen, *Angew. Chem. Int. Ed.* **2023**, *62*, e202304454.
[10] X. Liu, J. Wang, P. Lv, Y. Zhang, J. Li, Q. Wei, *Energy Storage Mater.* **2024**, *69*, 103382.
[11] R. Ma, Z. Xu, X. Wang, *Energy Environ. Mater.* **2023**, *6*, e12464.
[12] C.-C. Kao, j. liu, C. Ye, s.-j. zhang, J. Hao, S. Qiao, *J. Mater. Chem. A.* **2023**, *11*, 23881–23887.
[13] J. Zhao, C. Song, S. Ma, Q. Gao, Z. Li, Y. Dai, G. Li, *Energy Storage Mater.* **2023**, *61*, 102880.
[14] H. Zheng, Y. Huang, J. Xiao, W. Zeng, X. Li, X. Li, M. Wang, Y. Lin, *Chem. Eng. J.* **2023**, *468*, 143834.
[15] M. Jiao, L. Dai, H.-R. Ren, M. Zhang, X. Xiao, B. Wang, J. Yang, B. Liu, G. Zhou, H.-M. Cheng, *Angew. Chem. Int. Ed.* **2023**, *62*, e202301114.
[16] H. Wang, Y. Chen, H. Yu, W. Liu, G. Kuang, L. Mei, Z. Wu, W. Wei, X. Ji, B. Qu, *Adv. Funct. Mater.* **2022**, *32*, 2205600.
[17] J. A. Sánchez-Márquez, R. Fuentes-Ramírez, I. Cano-Rodríguez, Z. Gamiño-Arroyo, E. Rubio-Rosas, J. M. Kenny, N. Rescignano, *Int. J. Polym. Sci.* **2015**, *2015*, 320631.
[18] M. Zhu, X. Wang, H. Tang, J. Wang, Q. Hao, L. Liu, Y. Li, K. Zhang, O. G. Schmidt, *Adv. Funct. Mater.* **2020**, *30*, 1907218.
[19] M. Jiao, L. Dai, H.-R. Ren, M. Zhang, X. Xiao, B. Wang, J. Yang, B. Liu, G. Zhou, H.-M. Cheng, *Angew. Chem. Int. Ed.* **2023**, *135*, e202301114.
[20] P. Zhang, K. Wang, Y. Zuo, M. Wei, H. Wang, Z. Chen, N. Shang, P. Pei, *Chem. Eng. J.* **2023**, *451*, 138622.
[21] M. Zhou, S. Guo, J. Li, X. Luo, Z. Liu, T. Zhang, X. Cao, M. Long, B. Lu, A. Pan, G. Fang, J. Zhou, S. Liang, *Adv. Mater.* **2021**, *33*, 2100187.
[22] Q. Zhang, J. Luan, Y. Tang, X. Ji, H. Wang, *Angew. Chem. Int. Ed.* **2020**, *59*, 13180–13191.
[23] W. Deng, Z. Zhou, Y. Li, M. Zhang, X. Yuan, J. Hu, Z. Li, C. Li, R. Li, *ACS Nano* **2020**, *14*, 15776–15785.
[24] Z. Hu, D. Meng, Y. Wu, Y. Huang, L. Li, Z. Hong, *J. Power Sources* **2024**, *604*, 234465.
[25] L. Chen, T. Xiao, J.-L. Yang, Y. Liu, J. Xian, K. Liu, Y. Zhao, H. J. Fan, P. Yang, *Angew. Chem. Int. Ed.* **2024**, *63*, e202400230.
[26] H. Zhang, X. Gan, Y. Yan, J. Zhou, *Nano-Micro Lett.* **2024**, *16*, 106.

Manuscript received: December 10, 2024
Revised manuscript received: February 17, 2025
Accepted manuscript online: February 24, 2025
Version of record online: March 5, 2025